Studies in Surface Science and Catalysis 130
A. Corma, F.V. Melo, S. Mendioroz and J.L.G. Fierro (Editors)

Design of an SFG-compatible uhv-high pressure reaction cell: Studies of CO and NO adsorption on Ni and NiO(100) by IR-vis sum frequency generation vibrational spectroscopy

G. Rupprechter*, T. Dellwig, H. Unterhalt, and H.-J. Freund

Fritz-Haber-Institut der Max-Planck-Gesellschaft, Chemical Physics Department, Faradayweg 4-6, D-14195 Berlin, Germany

Optical infrared-visible sum frequency generation (SFG) vibrational spectroscopy is one of the few surface-specific techniques that can operate in a pressure range from ultrahigh vacuum to ambient conditions. Due to its inherent surface sensitivity and pressure independence, SFG is particularly suited for in-situ studies of adsorbates or surface species at elevated pressure or during a catalytic reaction. In this progress report we describe the design of an SFG-compatible elevated pressure reactor that is attached to an ultrahigh vacuum (uhv) surface analysis chamber. After preparation and characterization in uhv, model catalysts can be transferred in vacuo into the reaction cell. The reactor is separated from the uhv chamber by an arrangement of differentially pumped teflon seals. In order to test our system, we studied the adsorption of CO and NO on Ni and NiO(100) surfaces at low coverages.

1. INTRODUCTION

High pressure studies of catalytic processes on single crystal or uhv-grown model catalysts are frequently carried out using uhv-compatible reactor cells that are enclosed in or attached to a uhv surface analysis chamber. Utilizing this approach, introduced in the early 70's by Somorjai and coworkers [1], the model catalyst is characterized before the reaction in uhv by surface sensitive techniques, subsequently transferred into the reaction cell for high pressure catalysis (at about 1 bar), and finally analyzed in uhv after the reaction. Based on this concept, a number of research groups developed similar systems [e.g. 2-4].

However, in recent years it became apparent that it is important to study catalytically active surfaces under real reaction conditions and not just before and after the reaction. Adsorbed species present during a high pressure reaction may be different from those observed in a pre- or post-reaction analysis of surfaces in vacuum or at low pressure, as demonstrated for CO on Pt and Rh(111) [5,6]. Dominant species of low pressure studies may turn out to be mere spectators in the high pressure reaction. Several surface sensitive techniques have been developed that allow molecular level studies of surfaces under high pressure [6], among them IR-vis sum frequency generation surface vibrational spectroscopy.

In an effort to combine these two concepts, we have designed an apparatus that allows to prepare and characterize model catalysts under well-controlled conditions in uhv [7], and to monitor adsorbates at elevated pressure or during a catalytic reaction by *in-situ* SFG vibrational spectroscopy. The reaction rate and selectivity can be simultaneously determined by gas chromatography.

*corresponding author; rupprechter@fhi-berlin.mpg.de

Infrared-visible sum frequency generation is a surface-specific vibrational spectroscopy that can operate in a pressure range from uhv to ambient conditions and, hence, is able to bridge the gap to traditional surface science experiments. SFG is a second-order nonlinear optical process which involves the mixing of infrared (ω_{IR}) and visible light (ω_{vis}) to produce light at the sum of these two frequencies ($\omega_{SFG} = \omega_{IR} + \omega_{vis}$) [6,8]. To carry out an SFG experiment, the visible beam is held at fixed frequency while the infrared beam is tuned through the vibrational range of interest. An adsorbate spectrum is obtained by plotting the SFG intensity vs. the IR wavenumber. SFG is uniquely surface monolayer specific because such a non-linear process can occur only in media without inversion symmetry (in the electric-dipole approximation). The surface is such a medium and the dominant contribution is therefore generated by the modes of the adsorbed monolayer, while the bulk of most solids and the gas phase give nearly zero contribution to the signal.

To test and calibrate our system we have studied the adsorption of CO and NO on Ni and NiO(100) surfaces at low coverages. The results are compared to infrared reflection absorption spectroscopy (IRAS) and high resolution electron energy loss spectroscopy (HREELS) data.

2. EXPERIMENTAL

The experiments were performed in a two-level system that combines a uhv surface analysis chamber (base pressure 1×10^{-10} mbar, upper level) with an elevated pressure reactor (lower level) that is SFG- and uhv-compatible. With the help of an xyzφ manipulator with 400 mm z-travel, the sample can be transferred between the two levels while maintaining a uhv environment.

A sample holder (Fig. 1), which is basically a closed-end double-walled tube, is connected to the manipulator. A circular plate with four electrical feedthroughs (two Mo rods and a chromel-alumel thermocouple) is welded to the inside of the tube. The sample crystal is spotwelded to the Mo rods for resistive heating, and for temperature readings, a thin type K thermocouple is spotwelded to the rear of the crystal. After filling the inner tube with liquid N_2, a sample temperature of 85 K can be reached within 5 minutes. To avoid extensive cooling of the outside wall of the sample holder, the space in between the two tubes is evacuated. By resistive heating a temperature of 1300 K can be reached within minutes.

The Ni(100) single crystal was cleaned in the uhv chamber (upper level) by Ar ion bombardment (beam energy 1 kV at 2×10^{-4} mbar Ar) while heated to 850 K within 2 hours and annealed at 850 K for 2 minutes. The surface structure and cleanliness were examined by low energy electron diffraction (LEED), Auger electron spectroscopy (AES), and temperature programmed desorption (TPD). A NiO(100) surface was grown on Ni(100) as thin epitaxial film (3-5 nm) by repeated cycles of oxidation in 5×10^{-6} mbar O_2 at 573 K (5 min) and annealing at 650 K (2 min).

For vibrational studies and kinetic measurements, the specimen is transferred in vacuo into the SFG-compatible reaction cell (Fig. 1). When the manipulator is lowered to the SFG level, the sample holder is inserted into an arrangement of three differentially pumped spring-loaded teflon seals. The outside of the sample holder is mirror polished to provide a better sealing surface. The reaction cell can be pressurized to 1 bar without significantly degrading the vacuum in the uhv chamber. Fig. 1 shows a cross-section of the lower level of our chamber with the sample holder (inserted), the flange housing the teflon seals, and the reaction cell. The reactor is equipped with two CaF_2 windows to allow infrared and visible light to enter, and to allow sum frequency light to exit to the detector. The infrared and visible beams make an angle of 55° and 50° with respect to the surface normal, respectively, and overlap at the sample surface. Fig. 2 shows the orientation of the beams with respect to the reactor. The difference in the incident angles of the beams is necessary to spatially separate the SFG signal from the reflected pump beams. The source of the visible radiation (790 nm, 2 mJ/pulse, 2 ps, 500 Hz) is an amplified titanium sapphire laser, and part of the output is used to generate tunable infrared light (1-6 µm, ca. 10 µJ/pulse) with an optical parametric generator/amplifier (OPG/OPA). The flange between the CaF_2 windows is used as a gas inlet so that when catalytic reactions are carried out, the gas mixture is directed onto the catalyst surface (Fig. 2). Two flanges on the back of the reactor are used as gas outlet and, in batch mode, they are connected to a metal bellows recirculation pump. The recirculation loop is interfaced with a gas chromatograph through an electric gas sampling valve. To apply low exposures in uhv experiments, a leak valve and an ionization gauge are connected to a flange on the back of the reactor.

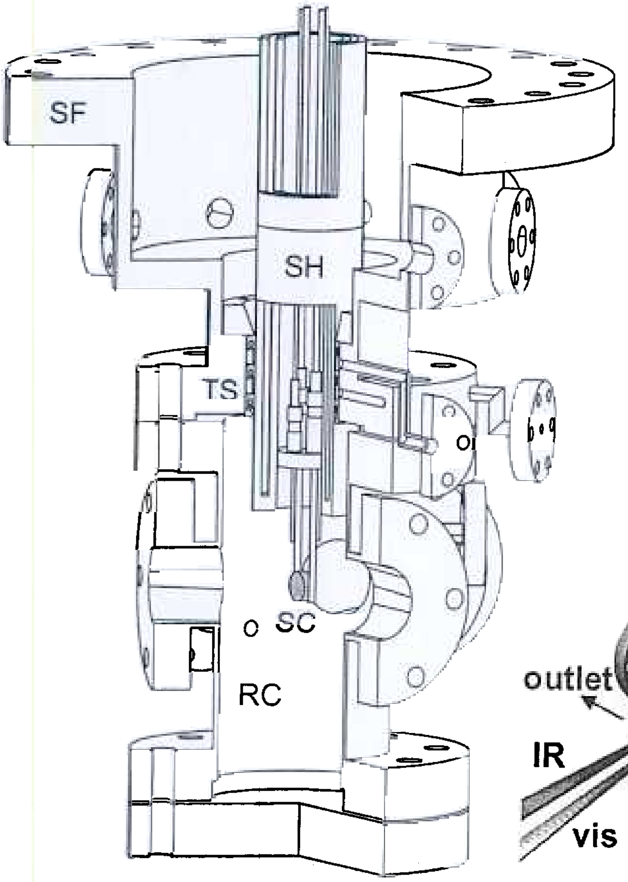

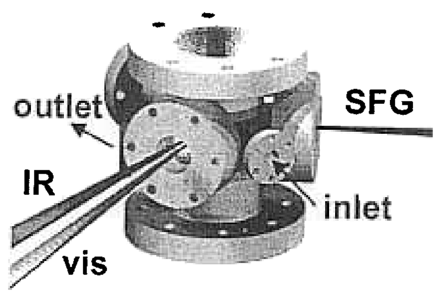

Figure 2
Alignment of the laser beams with respect to the reaction cell.

Figure 1 Cross-section displaying the sample holder (SH), the sealing flange (SF) housing the differentially-pumped spring-loaded teflon seals (TS), and the reaction cell (RC). A single crystal (SC) is spotwelded to the sample holder that is inserted into the teflon seals. To minimize background activity, the walls of the reaction cell are gold coated.

3. RESULTS

Nickel is a highly selective catalyst for the methanation of CO, and the promotion of C-O bond hydrogenation on supported Ni by the oxide-metal interface has received great attention. To better understand the properties of this catalyst, we have studied the adsorption of CO and NO on Ni(100) and on the corresponding ionic NiO(100) surface. In order to test our system and to compare the results with IRAS and HREELS data, our initial SFG experiments were performed under low pressure conditions.

As mentioned in section 2, the Ni(100) single crystal surface was cleaned by repeated sputter/anneal cycles and the cleanliness was checked by Auger electron spectroscopy. Carbon was the most resistant impurity (originating from bulk C segregation) because it occupies fourfold hollow sites on the surface and forms a very stable c(2x2) structure on Ni(100), as observed by LEED (Fig. 3) [9]. It has been reported that carbon species on Ni surfaces may act as precursor in the methanation reaction [10]. Remaining traces of surface carbon were removed by oxidation in 1 x 10^{-6} mbar O_2 at 570 K (5 min). After this treatment, oxygen was found on the surface by AES but could be removed by 1 x 10^{-6} mbar H_2 at 750 K (30 min) and a clean (1x1) surface was obtained. A CO-TPD spectrum of a Ni(100) surface is shown in Fig. 4. Upon adsorption of 0.5 L CO (1 Langmuir = 10^{-6} Torr sec), high binding energy adsorption sites at 420 K are occupied predominantly. Using the Redhead formula, the adsorption energy was estimated to be 110 kJ mol^{-1}. Higher CO exposures reduce the desorption temperature of this species up to 10 K due to repulsive interactions between CO molecules that decrease the heat of adsorption. Exposures >1 L produce additional desorption peaks around 350 and 280 K. At coverages $\leq$ 0.5 ML (~ 2 L), CO forms an ordered c(2x2) structure but at higher coverages a compressed overlayer is formed. This makes the desorption process rather complicated [11], which is reflected by the emergence of the low temperature peaks at high coverages. The 420 K desorption peak was found to be at least equally sensitive to surface carbon as Auger spectroscopy. Carbon in fourfold hollow sites seems to hinder the adsorption of CO on the high binding energy sites while the broad peaks at 280 and 350 K were less affected. When the 420 K peak was absent, i.e. when carbon was present, no adsorbates could be detected by SFG.

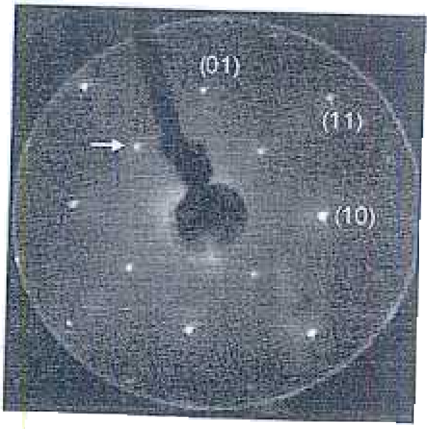

igure 3 LEED pattern of Ni(100) c(2x2)C 100 K (125 eV). One carbon spot is arked by an arrow.

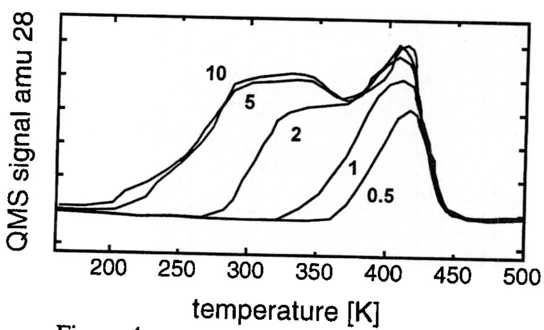

Figure 4
TPD spectra for different CO exposures on Ni(100) at 100 K collected at a heating rate of 2 K s^{-1} (exposure indicated in Langmuirs).

SFG spectra of CO adsorption on Ni(100) at 100 K for different exposures are shown in Fig. 5. For comparison of our results with data from infrared reflection absorption spectroscopy (IRAS) and high resolution electron energy loss spectroscopy (HREELS), low exposures were used in our studies, since the IRAS and HREELS experiments were carried out at low pressure. The nonlinear SFG response from the clean Ni(100) surface was constant between 1950 and 2200 cm^{-1}. After exposing Ni(100) at 100 K to 0.5 L CO (i.e. ~ 0.1 ML [12]) a single resonance feature characteristic of the stretching vibration of terminally bonded (on-top) CO was observed. The desorption peak at 420 K is therefore attributed to on-top CO, while the lower temperature peaks are rather connected to the compressed overlayer. This is supported by the consideration that carbon in fourfold hollow sites strongly interferes with atop Ni sites and hence prevents linear bonding. The absence of bridge-bonded CO in our spectra is probably due to the small IR intensity of our current setup below 2000 cm^{-1}.

With increasing CO coverage the frequency of the CO peak shifted from 2017 cm^{-1} at 0.5 L (~ 0.1 ML), to 2030 cm^{-1} at 1 L (~ 0.25 ML), to 2036 cm^{-1} at 2 L (~ 0.5 ML; c(2x2)), and to 2063 cm^{-1} at 10 L (~ 0.7 ML). As the packing density of CO increases, there is an enhancement in the dipole coupling between the CO molecules on the surface and a weakening of their bonds to the metal (cf. Fig. 4), resulting in the observed frequency shift. The shift up to $\theta = 0.5$ is in good agreement with previous IRAS, HREELS and SFG studies [8, 12-16]. At coverages > 0.5, the IRA and EEL spectra in refs. [12,13] exhibit a broad band between 2000 and 2100 cm^{-1}, indicating that a distinct terminal site no longer exists. It has been suggested that CO molecules are arranged in incommensurate adsorbate layers, similar to the situation found for CO on Pt(111) above 150 mbar [6]. The SFG spectra that we aquired at saturation coverage of CO (e.g. 10 L) did not show a broad band but still exhibited a peak at 2063 cm^{-1}. A similar result was obtained in an EELS study by Uvdal et al. [14] who observed both on-top and bridge sites at $\theta = 0.6$ and in an FT-IRAS study by Ibach [15]. The presence of a distinct on-top CO peak at $\theta > 0.5$ supports the coincidence structure models suggested by Biberian and van Hove [17] for the compressed overlayer, since these models allow to place CO molecules in well-specified on-top and bridge sites. It seems likely that the influence of even small amounts of carbon impurities may account for the different adsorption geometries reported in the literature.

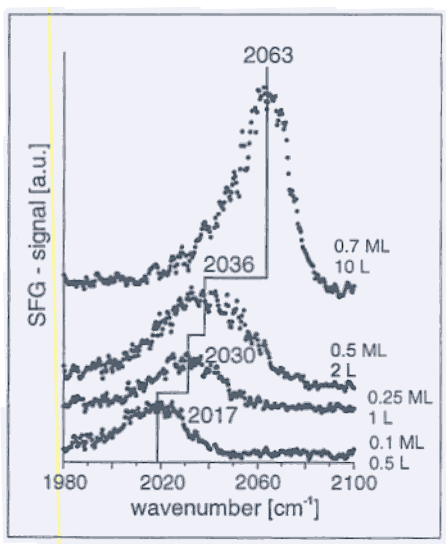

Figure 5
SFG spectra of CO adsorption on Ni(100) at 100 K for different exposures.
The observed resonance feature is characteristic of terminally bonded (on-top) CO.

On NiO(100), upon similar exposures, the on-top CO peak appeared closer to the gas phase value, indicating weaker bonding of CO to NiO(100) as compared to Ni(100) [18]. This was corroborated by the measured desorption temperatures of CO; around 200 K on NiO and around 420 K for the metal. The SFG signal of NO on NiO(100) at 1780 cm^{-1} was weak due to the tilted geometry of the N-O bond [18], which is unfavorable according to the SFG selection rule, and due to a low infrared energy in this spectral region.

It was recently shown for Pt and Rh(111) that the adsorption site occupancy at high pressure may be different from what is observed under low pressure [5,6]. Weakly bound adsorbates that are absent in uhv studies may turn out to be the active species in the high pressure reaction. Atmospheric pressures of CO restructure the Rh surface, and a CO species bound to defect sites was detected. High pressure studies on Ni are difficult due to the fast dissociation of CO, rapid carbon contamination and the formation of volatile Ni-carbonyls. Our recent adsorption studies on Pt and Pd up to 500 mbar CO will be presented elsewhere.

4. CONCLUSIONS

We have set up an instrument that enables us to prepare and characterize well-defined model catalysts in uhv, and to transfer them in vacuo into an SFG-compatible elevated pressure reactor. Preliminary studies of CO adsorption on Ni(100) indicate that CO adsorbs on on-top sites at coverages ≤ 0.5 ML, and favor the coincidence structure models for higher coverages. On NiO(100), the C-O stretching frequency was found close to the C-O gas phase value, as a result of the weak interaction with the oxidic substrate, while the N-O stretching frequency was shifted to lower wavenumbers due to the chemical bonding to the surface. At present, we are setting up a new OPG/OPA system to improve our resolution and to obtain more IR-power below 2000 cm^{-1}. The reaction cell is fully uhv compatible and can be pressurized to 1 bar while the uhv analysis system can still be kept at 5×10^{-10} mbar. Studies of adsorption and reactions at higher pressure are in progress.

REFERENCES

1. D.W. Blakely, E. Kozak, B.A. Sexton, G.A. Somorjai, J. Vac. Sci. Technol., 13 (1976) 1091.
2. D.W. Goodman, R.D. Kelley, T.E. Madey, J.T. Yates, J. Catal., 63 (1980) 226.
3. R.A. Campbell, D.W. Goodman, Rev. Sci. Instrum., 63 (1992) 172.
4. C. Sellmer, A. Gaussmann, N. Kruse, R. Prins, J. Vac. Sci. Technol. A, 15 (1997) 365.
5. X. Su, P.S. Cremer, Y. R. Shen, G.A. Somorjai, Phys. Rev. Lett., 77 (1996) 3858.
6. G. A. Somorjai, G. Rupprechter, J. Phys. Chem. B, 103 (1999) 1623.
7. H.-J. Freund, Angew. Chem. Int. Ed., 36 (1997) 452.
8. J. Miragliotta, P. Rabinowitz, S.D. Cameron, R.B. Hall, Appl. Phys. A, 51 (1990) 221.
9. G. A. Somorjai, G. Rupprechter, J. Chem. Edu., 75 (1998) 161.
10. D. Kelley, D.W. Goodman, in: Chem. Physics Sol. Surf. Het. Catal., 4 (1982) 435.
11. S. Johnson, R.J. Madix, Surf. Sci., 108 (1981) 77.
12. J. Lauterbach, M. Wittmann and J. Küppers, Surf. Sci., 279 (1992) 287.
13. S. Andersson, Solid State Comm., 88 (1993) 1085.
14. P. Uvdal, P.-A. Karlsson, S. Andersson, N.V. Richardson, Surf. Sci., 202 (1988) 167.
15. A. Grossmann, W. Erley, H. Ibach, Surf. Sci., 330 (1995) L646.
16. J. Yoshinobu, M. Kawai, Surf. Sci., 363 (1996) 105; Surf. Sci., 368 (1996) 239.
17. J.P. Biberian, M.A. van Hove, Surf. Sci., 118 (1982) 443.
18. M. Schönnenbeck, D. Cappus, H.-J. Freund et al., Surf. Sci., 347 (1996) 337.